Thermal Analysis of Novel Underfill Materials with Optimum Processing Characteristics

Yang Liu,[1] Yi-Feng Wang,[2] Timofey G. Gerasimov,[1] Kenneth H. Heffner,[3] Julie P. Harmon[1]

[1]*Department of Chemistry, University of South Florida, Tampa, Florida 33620*
[2]*Cyclics Corporation, Schenectady, New York 12308*
[3]*Honeywell Corporation, Clearwater, Florida, 33764*

Received 8 October 2004; accepted 1 February 2005
DOI 10.1002/app.22272
Published online in Wiley InterScience (www.interscience.wiley.com).

ABSTRACT: This work encompasses the development of low-viscosity cyclic oligomer underfill formulations that cure without heat evolution. Boron nitride, silica-coated aluminum nitride, and alumina ceramic powders were used as fillers in cyclic butylene terephthalate oligomer melts. The melts were heated with a suitable catalyst to induce polymerization. The effects of the filler type and composition on the thermal and mechanical properties of the poly(butylene terephthalate)/filler composites were examined with differential scanning calorimetry, temperature-modulated differential scanning calorimetry, thermogravimetric analysis, thermomechanical analysis, and dynamic mechanical analysis. Scanning electron microscopy was employed to elucidate the morphology of these composites. © 2005 Wiley Periodicals, Inc. J Appl Polym Sci 98: 1300–1307, 2005

Key words: differential scanning calorimetry (DSC); fillers; thermal properties

INTRODUCTION

Technology development in microelectronics has led to high-packing-density devices that exhibit reduced weight and height profile, shorter interconnection length, higher electrical performance, improved reliability, better manufacturability, and lower cost.[1–4] However, the mismatch in the coefficient of thermal expansion (CTE) between the substrate and silicon chip still poses a significant challenge. The coefficients of thermal expansion of a typical silicon chip, substrate, and solder are 2.3–2.5, 18–25, and 25–26 μm/m/°C, respectively.[4–6] Because of the CTE mismatch, thermal stress occurs on the solder joints, resulting in fatigue and crack growth during temperature cycling.[7] The current method for overcoming these challenges is to use a composite polymeric underfill material.[8–12] The underfill provides mechanical reinforcement, redistributes thermal stress on the solder joints, minimizes the CTE mismatch between the substrate and the die, and protects the chips from moisture, ionic contamination, and radiation.[8–10,13] The use of underfill material offers additional protection against hostile operating environments, such as mechanical pull, shear, twist, shock, and vibration.

Another important application of underfill materials originates from their improved thermal conductivity,[14–18] which increases the heat transport from the silicon chip. Polymers are thermally insulating materials; the thermal conductivity of a typical polymer is less than 0.3 W/m K.[19] The use of fillers to enhance the thermal conductivity of polymeric compounds has been studied extensively. Thermally conducting but electrically insulating fillers such as diamond micropowder, boron nitride (BN), aluminum nitride, silicon carbide, alumina (Al_2O_3), and silicon-coated aluminum nitride are used to increase the thermal conductivity of polymer matrices.[4,13–23] Efficient underfill materials have thermal conductivity values in a range of 1.3–4 W/m K.[19] Recently, Ishida and Rimdusit[14] reported the use of low-melt-viscosity polybenzoxazine filled with BN ceramics to improve the composite thermal conductivity up to 32.5 W/m K at the maximum filler loading of 78 vol %.

Polymer melts possess high viscosities even when heated to high temperatures. This prevents filler materials from being finely dispersed in a polymer matrix and limits filler concentration. One possible solution to this problem is the use of low-viscosity monomers or oligomers. It has been reported that cyclic butylene terephthalate (CBT) resins are compatible with a variety of standard fillers allowing for high filler loadings of 80 vol % or greater.[24,25] When mixed with specific tin or titanium polymerization catalyst, the CBT rings open to form high-molecular-weight poly(butylene terephthalate) (PBT) without an exotherm or offgassing. The polymerization usually reaches completion

Correspondence to: J. P. Harmon.
Contract grant sponsor: Honeywell Corporation.
Contract grant sponsor: Florida High Tech Corridor Initiative.

TABLE I
Characteristic Properties of the Pure PBT and Pure Fillers Used in This Study

Material	PBT	AN	Al_2O_3	BN
Density (g/cm^3)	1.37	3.26	3.98	2.25
Thermal conductivity (W/mK)	0.16	220	30	250–300
CTE ($\mu m/m/°C$)	144	4.4	6.6	<1
Young's modulus (GPa)	2.5–3	330	385	75–90
Dielectric Constant (at 20°C)	3	8.8	9.7	3.9
C_p (J/Kg)	1.12	0.734	0.798	0.794

Cp = specific heat capacity at constant pressure.

in several minutes, the time depending on the temperature and the type of catalyst used.[24,25]

The objective of this study was to evaluate CBT oligomers blended with BN, silica-coated aluminum nitride (AN), and Al_2O_3 and subsequently polymerized to yield PBT composites as possible underfill materials. The effects of the filler type and composition on the composite thermal and mechanical properties as well as morphology were examined. The crystallization and melting behavior of the underfill materials were characterized via differential scanning calorimetry (DSC), whereas the glass-transition temperatures were identified by temperature-modulated DSC. Dynamic mechanical analysis (DMA) measured the viscoelastic response of a material under a periodic load. The modulus values provided an indication of material stiffness, whereas mechanical damping correlated with the amount of energy dissipated during the deformation of the material. A systematic investigation of the relaxation spectra predicted the structure of the materials and obtained the transition-temperature profiles for different types of polymer relaxations. Thermomechanical analysis (TMA) was used to evaluate the thermal expansion of the pure polymer and composite materials. Thermogravimetric analysis (TGA) was used to characterize the decomposition temperatures of neat and filled PBT as well as the filler load. A detailed thermal conductivity study will be the subject of a forthcoming article.

EXPERIMENTAL

Fillers

The fillers used in this study included AN (SCAN70, Dow Chemical, Midland, MI), three BN samples (AS1065, Carburundum Co. Niagara Falls, NY, and PT140S and PT180S, Advanced Ceramics Co., Cleveland, OH), and Al_2O_3 and nano-Al_2O_3 (Inframet Corp., Farmington, CT). All fillers were dried at 140°C *in vacuo* for 24 h before use. The important characteristics of the fillers are listed in Table I. The average particle sizes varied for different Al_2O_3 and BN samples.

Sample preparation

Cyclic (butylene terephthalate) (CBT) oligomers complexed with a catalyst were obtained from Cyclics Corp. (Schenectady, NY). The CBT powder was heated at 90°C *in vacuo* for 3 h to remove the moisture. The dried powder was mixed with fillers for 5–10 min. A constant filler loading of 20 wt % was used for all the samples. The premixed samples were heated to 190°C for 10 min. Then, pressure was applied to the mold for 1 h at 190°C to yield the linear, chain-extended PBT. The samples were air-cooled under pressure and subsequently demolded as wafer samples 2.4 cm in diameter and 0.8 cm thick. PBT samples with different crystallinity levels were prepared by the annealing of PBT at 190°C for an additional 2 and 16 h. Another sample was prepared by the quenching of polymerized PBT with liquid nitrogen. The notations for all the prepared samples are listed in Table II. These notations are used throughout the article.

Apparatus

Gel permeation chromatography (GPC)

The molecular weight of pure PBT samples was analyzed by GPC with polystyrene as a standard. An Agilent 1100 series high-performance liquid chromatograph

TABLE II
PBT Sample Compositions, Polymerization Conditions, and Filler Particle Sizes

Sample	Sample composition	Filler particle size* (μm)[a]	Annealing time (h)	Cooling
PBT(0)	Pure PBT	N/A	0	Air
PBT(2)	Pure PBT	N/A	2	Air
PBT(16)	Pure PBT	N/A	16	Air
PBT(Q)	Pure PBT	N/A	0	Liquid nitrogen
ALO(10–20)	20 wt % Al_2O_3 in PBT	10–20	0	Air
ALO(nano)	20 wt % Al_2O_3 in PBT	0.15	0	Air
AN(10–20)	20 wt % SCAN70 in PBT	10–20	0	Air
BN(5–11)	20 wt % PT140S in PBT	5–11	0	Air
BN(8–14)	20 wt % PT180S in PBT	8–14	0	Air
BN(52)	20 wt % AS1065 in PBT	52	0	Air

[a] Average particle size as reported by filler manufacturers.
[b] Only the coarsest particle size was available.

(Brockville, Canada) equipped with a UV detector was used to measure the molecular weight of PBT. Two Phenomenex Phenogel 5-μm linear columns (300 $\times$ 7.80 mm, 5 μm; Torrance, CA) were used in series. A solvent mixture of hexafluoroisopropanol and methylene chloride was used to dissolve PBT and then diluted with chloroform for GPC analysis. Chloroform was the eluant for the GPC run. The average values of the number-average and weight-average molecular weights, determined by Cyclics, for the pure PBT samples were 45,000 and 149,000 g/mol, respectively.

DSC

A DSC 2920 differential scanning calorimeter (TA Instruments, New Castle, DE) was used to characterize the thermal behavior of the samples. Dry nitrogen gas with a flow rate of 75 mL/min was purged through the sample cell. Cooling was accomplished with a liquid nitrogen cooling accessory. Indium was used for temperature calibration. The heat capacity calibration was carried out with a 24.9-mg sapphire. For all conventional DSC experiments, a temperature ramp of 5°C/min was used. Temperature-modulated DSC experiments were conducted under the following conditions: a temperature ramp of 3°C/min, a temperature modulation amplitude of 1°C, and a modulation period of 60 s were used throughout the temperature range of -50 to 150°C.

DMA

A 2980 dynamic mechanical analyzer (TA Instruments) was used in the tension film mode to obtain the reported mechanical data. The temperature range of each analysis was -150°C to the temperature at which the sample yielded. A TA Instruments liquid nitrogen cooling accessory was used to control the heating rate at 4°C/min.

Scanning electron microscopy (SEM)

The morphologies of the fractured surfaces of the composites with the fillers in the PBT matrix were observed with a Hitachi S800 scanning electron microscope (Hitachi, Pleasanton, CA). The fracture surfaces were coated with 10-nm thin films of an evaporated gold/palladium alloy. The applied voltage depended on the magnification.

TMA

TMA was performed on a DuPont Instruments TMA 2940 (New Castle, DE). The samples were pressed into pellets 3 mm in diameter and 0.6 mm thick. All samples were heated from 25 to 150°C with a heating rate of 5°C/min and a loading force of 0.005 N. CTE (μm/m/°C) for each sample was determined at 100°C.

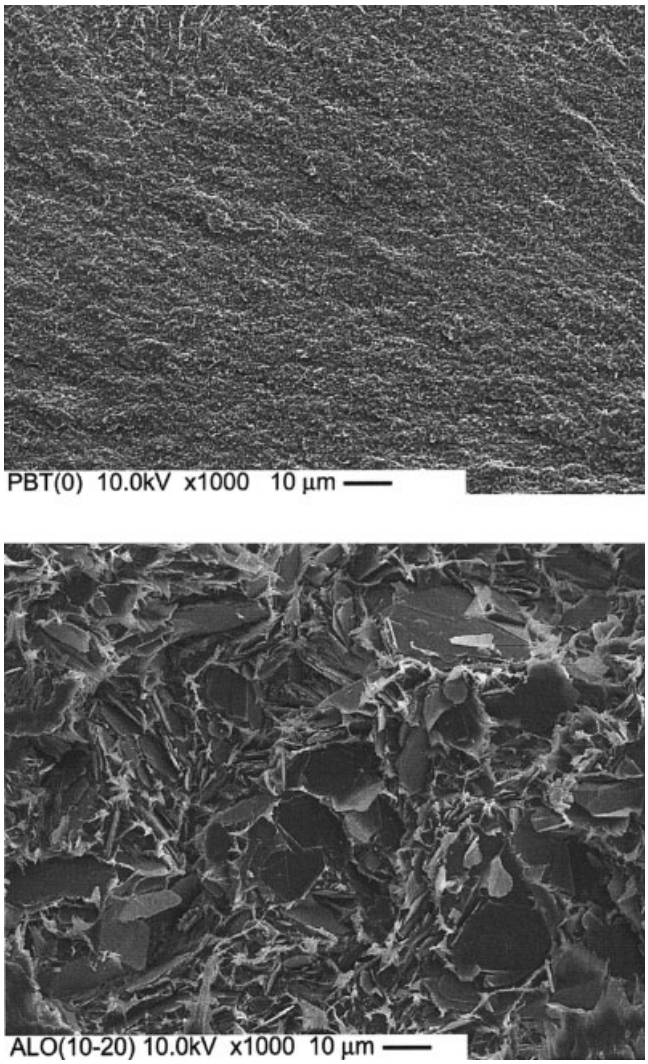

Figure 1 SEM images of samples of PBT(0) and ALO(10–20).

TGA

The decomposition process of the composites specimens from 25 to 570°C in an air atmosphere was determined with a Dupont Instruments 951 thermogravimetric analyzer. The heating rate was 5°C/min.

RESULTS AND DISCUSSION

SEM imaging

CBT oligomers are solid at room temperature; they fully melt above 150°C and exhibit viscosities of about 150 cP. The viscosity decreases to less than 20 cP at 180°C. The initial waterlike viscosity allows for rapid and excellent dispersion of fillers and fiber reinforcements. The optimum dispersion of fillers was confirmed by SEM. Figure 1 shows the SEM micrographs of the fracture surfaces of PBT(0) and ALO(10–20). The fillers are dispersed in the PBT matrix. The size of the filler particles ranges between several micrometers and tens of micrometers. Some of the filler particles

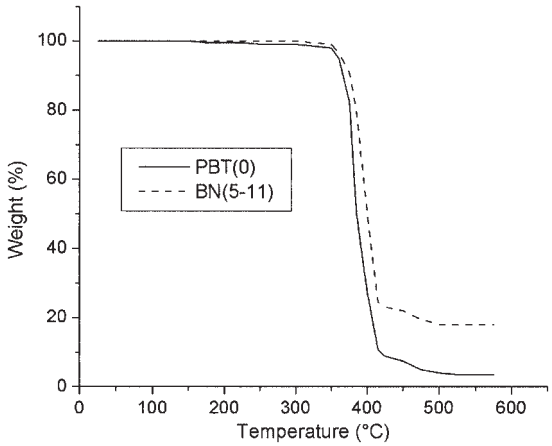

Figure 2 TGA plot of PBT(0) and composite BN(5–11).

pile up together, and this can facilitate the thermal conductivity of the PBT matrix.

Weight-loss profile and filler content (TGA)

The filler content of the underfill can be easily determined by TGA. TGA plots showing the total weight loss upon the heating of PBT(0) and BN(5–11) samples to 570°C are shown in Figure 2. The degradation of the underfill material has only one major stage. The onset temperature of the degradation stage for all the samples is 370°C, and this demonstrates the excellent thermal stability of PBT-based underfill materials. The residual weights of all thermally treated samples match closely the known amounts (20 wt %) of the fillers that were added to each cyclic oligomer sample.

DSC data

DSC measurements provide qualitative and quantitative information as a function of the time and temperature regarding transitions in materials that involve endothermic or exothermic processes or changes in the heat capacity. DSC curves of PBT and PBT with fillers in the heating–cooling process for the melt-crystallized samples were obtained at a heating rate of 5°C/min. Figure 3 shows DSC curves for PBT(0) and the ALO(10–20) composite. Although the melting points were determined by the conventional DSC technique, it was necessary to apply temperature-modulated DSC to elucidate the positions of the glass-transition temperatures.[26] Reversing curves in temperature-modulated DSC exhibit well-defined glass-transition temperatures in filled and semicrystalline samples, as depicted in Figure 4. The setup for temperature-modulated DSC is discussed in the Experimental section of this article. The glass-transition temperatures, melting points, and crystallization temperatures for the first and second heating cycles as well as the degrees of crystallinity for all samples are shown in Table III.

The effect that the degree of crystallinity has on the thermal properties of pure PBT was investigated. A set of four PBT samples with different crystallinity levels was prepared, as described in the Experimental section. The heat of fusion of 142 J/g for the perfect PBT crystals was reported by Illers.[27] The degree of crystallinity for PBT was calculated from heating curves via the ratio of the heat associated with melting to the heat of fusion for 100% crystalline PBT. As expected, the samples showed an increase in the melting points as the crystallinity increased.

The melting points of the PBT/filler composites were slightly lower and the crystallization temperatures were higher than those of pure PBT(0) for the first heating cycle. The degrees of crystallinity of the filled samples calculated from DSC data varied from 27.5 to 48.5% in the first heating cycle and from 34.2 to 44.1% in the second heating cycle. The ALO(nano) sample exhibited the lowest degree of crystallinity.

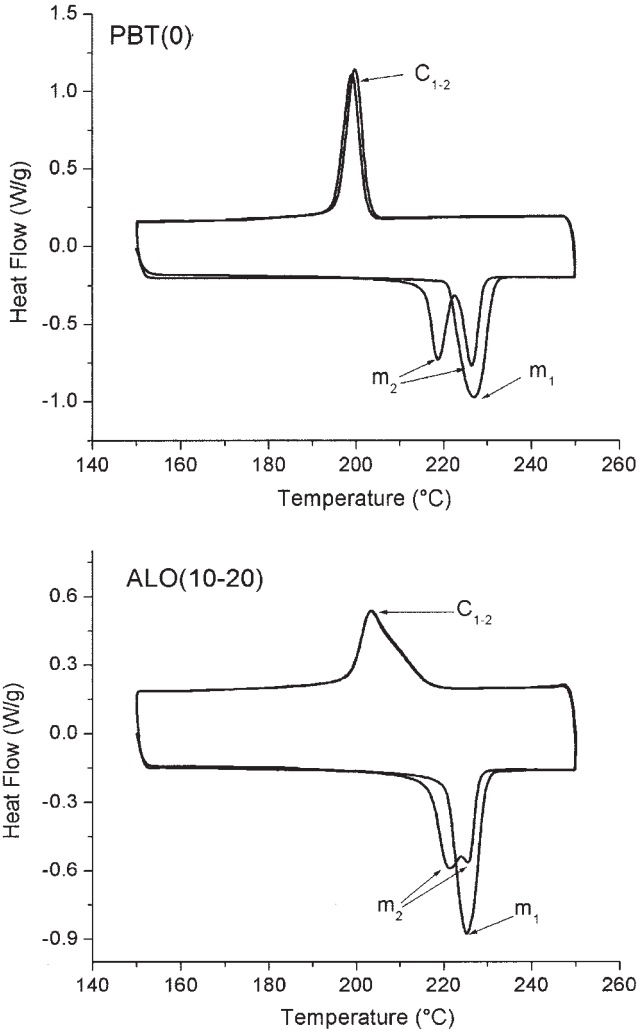

Figure 3 Melting and crystallization curves of PBT(0) and ALO(10–20). The scanning rate was 5°C/min. m_1 is a first heating cycle melting peak, m_2 is a second heating cycle melting peak, and C_{1-2} is a crystallization peak.

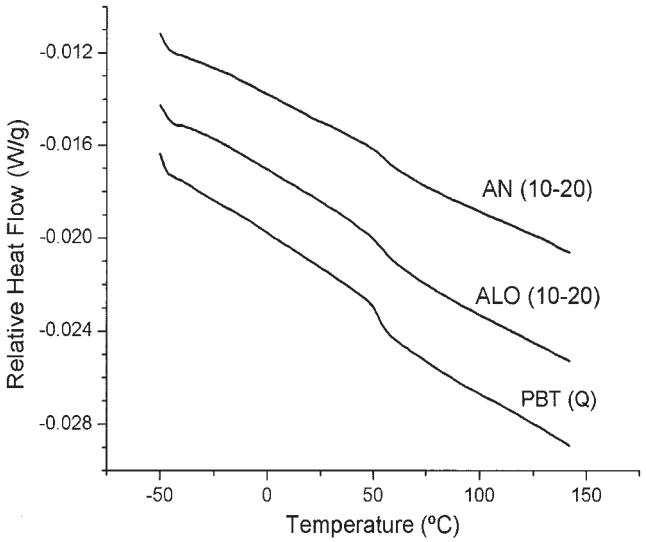

Figure 4 Thermograms showing reversing heat flow curves and glass-transition temperatures for PBT(Q), ALO(10–20), and AN(10–20).

This may be explained by the high surface area of the nanofiller, which disrupted crystal growth in a greater number of polymer chains at the filler–polymer interface.

All the samples, except for BN(8–14), exhibited a similar trend, with one melting peak appearing during the first heating cycle and double melting peaks appearing during the second and higher heating cycles. The double melting behavior of PBT is well known. Possible explanations, proposed by different research groups, include the following:

- The melt-recrystallization model.[28–30] This attributes the low-temperature melting peak to the melting of some amount of original crystals and the high-temperature melting peak to the melting of crystals formed by the melt-recrystallization process during the heating scan.
- The bimodal distribution of melting points.[31,32] This occurs when the PBT sample is crystallized during cooling.
- Different types of spherulites.[33,34] There are two different types of spherulites[35–38] for PBT crystals, one showing a normal Maltese cross and the other a Maltese cross rotated 45° in comparison with the normal position.

The double melting behavior of filled PBT samples is much less pronounced than that of pure PBT. This may be explained by the broadening and overlapping of individual melting peaks typical for the polymers when impurities (fillers in this case) are present. The different natures, sizes, and surface areas of the fillers affect the extent of peak broadening and therefore the observed melting temperatures.

Only one exothermic (crystallization) peak was observed in the DSC curves for all samples. The single exothermic peak suggests that a single-mode distribution in the crystallization size was formed during the cooling process.

Analysis of CTE

A thorough analysis of CTE of underfill materials is an important part of this study because of the pronounced effect that such properties have on thermal stresses in microchip packaging.[3] Such thermal stresses arise during both processing and use because of the mismatch in CTEs of the structural components of the assembly.

The effect that the degree of crystallinity has on CTE of PBT was investigated. A set of four PBT samples with different crystallinity levels was prepared. The CTE and crystallinity values are shown in Tables III

TABLE III
DSC Data for the PBT-Based Underfill Materials

	First heating cycle				Second heating cycle			
Sample	T_g (°C)	T_m (°C)	T_c (°C)	Degree of crystallinity (%)	T_{m1} (°C)	T_{m2} (°C)	T_c (°C)	Degree of crystallinity (%)
PBT(0)	48.7	227.0	199.7	43.7	218.3	226.0	198.3	38.2
PBT(2)	53.5	229.3	196.2	49.8	219.5	226.6	195.8	38.5
PBT(16)	57.1	231.8	199.1	50.2	219.3	227.3	199.3	38.4
PBT(Q)	52.2	227.3	195.3	38.2	219.8	226.0	194.9	35.1
ALO(10–20)	56.0	225.2	203.5	44.2	221.7	225.4	203.3	39.0
ALO(nano)	40.0	216.0	198.4	27.5	219.0	224.5	203.2	34.2
AN(10–20)	53.2	225.6	202.9	48.5	219.8	225.5	203.7	44.1
BN(5–11)	42.9	225.0	203.8	41.4	219.5	225.4	204.5	40.1
BN(8–14)	53.1	226.0	207.8	40.7	—	225.1	207.9	42.0
BN(52)	52.5	221.2	203.9	43.4	222.0	225.4	205.9	37.7

T_g = glass transition; T_m = melting transition in first heating; T_{m1} = lower melting peak in second heating; T_{m2} = higher melting peak in second heating cycle; T_c = crystallization temperature.

TABLE IV
Thermal and Mechanical Properties of PBT-Based Underfill Materials

Sample	CTE at 100°C (μm/m/°C)	Storage modulus at 0°C (MPa)	γ and β-transition temperature at 1 Hz and activation energy (E_a)			
			γ(°C)	E_a (kJ/mol)	β (°C)	E_a (kJ/mol)
PBT(0)	144.0	2875	−99.8	47.2	52.0	337.0
PBT(2)	111.4	4150	−103.8	52.9	52.8	—
PBT(16)	103.1	4171	−103.8	43.2	54.4	337.7
PBT(Q)	157.7	1737	−113.5	40.6	51.8	394.8
ALO(10–20)	140.7	5039	−109.0	51.4	52.0	384.6
ALO(nano)	156.4	4631	−116.0	70.6	29.4	356.0
AN(10–20)	133.2	4332	−106.0	47.7	54.4	335.0
BN(5–11)	129.5	4889	−102.0	57.8	48.0	405.8
BN(8–14)	69.8	4445	−99.8	63.7	49.6	443.4
BN(52)	56.7	4147	−99.2	58.1	48.8	427.9

and IV. CTE decreased with an increase in the crystallinity percentage, as shown in Figure 5.

The addition of ceramic fillers to a polymer matrix generally decreases CTE. The most significant change in CTE was observed for BN-filled samples [BN(52) and BN(81–14)]. CTE of the BN(52) composite was almost 2.5 times lower than CTE of the PBT(0) sample. This can be related to the CTE values of the pure fillers (Table I). Pure BN had the lowest CTE value (<1 μm/m/°C). However, the CTE values did not decrease significantly for the ALO(10–20) or AN(10–20) samples. The ALO(nano) sample had a CTE value slightly higher than that of the pure polymer. This coincided with the low crystallinity percentage (24.7%) of the ALO(nano) sample in comparison with that (43.7%) for PBT(0). Figure 6 shows a relative increase in the sample length (μm/m) for the PBT(0) sample in comparison with several selected samples. The CTE values measured at 100°C are shown in Table IV.

All of this indicates that the CTE values in filled semicrystalline composites depend on two factors: the intrinsic CTE values of the fillers and the degree of crystallinity in the polymer matrix. Therefore, it is possible to produce a composite with the desired CTE value by the adjustment of both the filler load and the annealing time.

Mechanical properties of PBT and PBT composites (DMA)

The dynamic mechanical properties of PBT-based composites were studied with DMA. The underlying thermal relaxations were identified, and their activation energies were estimated. Typical frequency-dependent relaxations that occur in PBT include the following:

1. The α transition near 225°C, which is due to the melting of PBT crystallites. This transition can-

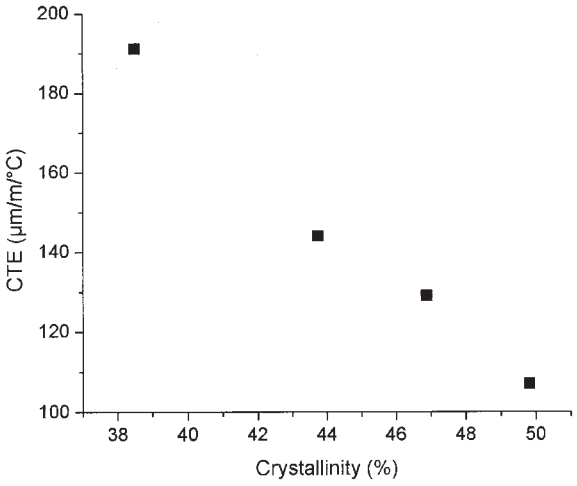

Figure 5 Plot of the crystallinity percentage of PBT versus CTE.

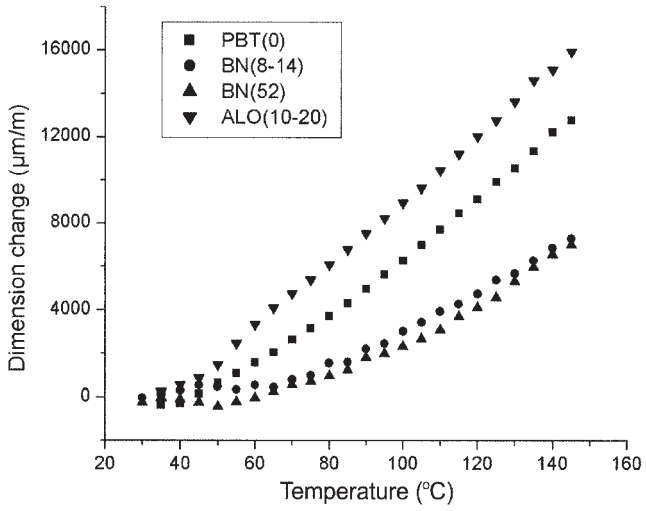

Figure 6 Dimensional changes (ppm) for (■) PBT(0), (●) BN(8–14), (▲) BN(52), and (▼) ALO(10–20) samples heated at 5°C/min.

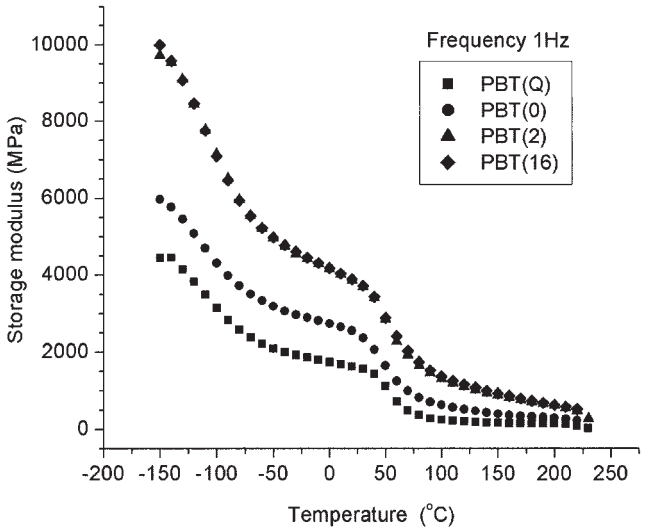

Figure 7 Storage modulus of PBT with different crystallinities at 1 Hz.

not be seen with DMA because of the sample melting.[39]

2. The β transition at about 50°C, which is attributed to the micro-Brownian motion of the polymer chains and is associated with the glass-transition temperature.[39]
3. The γ transition at about −100°C, which is a secondary relaxation associated with the superposition of several processes involving most likely the motion of the —O—$(CH_2)_4$—O— group,[40] the glycol (OH) residue in the noncrystalline phase,[41] or the carbonyl (COO) residue.[42]

The modulus curves of PBT polymer samples are affected by both the degree of crystallinity and the filler incorporated into the polymer matrix. The effects of the degree of crystallinity are usually described in the literature by two mechanisms.[43] First, the crystallites act as crosslinks by tying segments, especially amorphous molecules, together. Second, the crystallites have very high moduli in comparison with the rubbery, amorphous parts. Thus, they act just like rigid fillers in an amorphous matrix. To research these effects, four samples with different degrees of crystallinity were fabricated, as described in the Experimental section. The results are shown in Table IV. Figure 7 shows the storage moduli at 1 Hz of the PBT samples with different crystallinities. The liquid-N_2-quenched sample [PBT(Q)] had the lowest crystallinity level and the lowest storage modulus. The difference in the crystallinity percentages between the two annealed samples is not significant. As a result, the storage modulus data obtained for both annealed samples are close throughout the whole temperature range up to the melting point.

The storage moduli of PBT and PBT with fillers at 0°C are shown in Table IV. At −150°C, the storage moduli of ALO(10–20) and AN(10–20) were 2 and 1.5 times higher than the one without fillers. As the temperature increased, the difference between the filled and neat PBT samples decreased. Figure 8 shows the storage and loss modulus of PBT(0) and selected composites at 1 Hz with filler loadings of 20 wt %. The difference in the composite modulus corresponds to the difference in the modulus of the fillers (Table I). Al_2O_3 had the highest modulus, whereas BN had the lowest one. Likewise, the Al_2O_3-filled composites possessed a higher storage modulus, and the BN-filled composites had the lowest modulus.

The activation energies for the β transitions and γ transitions for all the samples were calculated from the Arrhenius temperature dependence[43] of $\ln f$ versus $1/T$, where T refers to the temperature of the maximum loss modulus at a fixed frequency f. Both the glass transitions (β) and γ transitions exhibited Arrhenius behavior. In amorphous polymers, glass-transition relaxation behavior is generalized by the Williams–Landel–Ferry equation:[44,45]

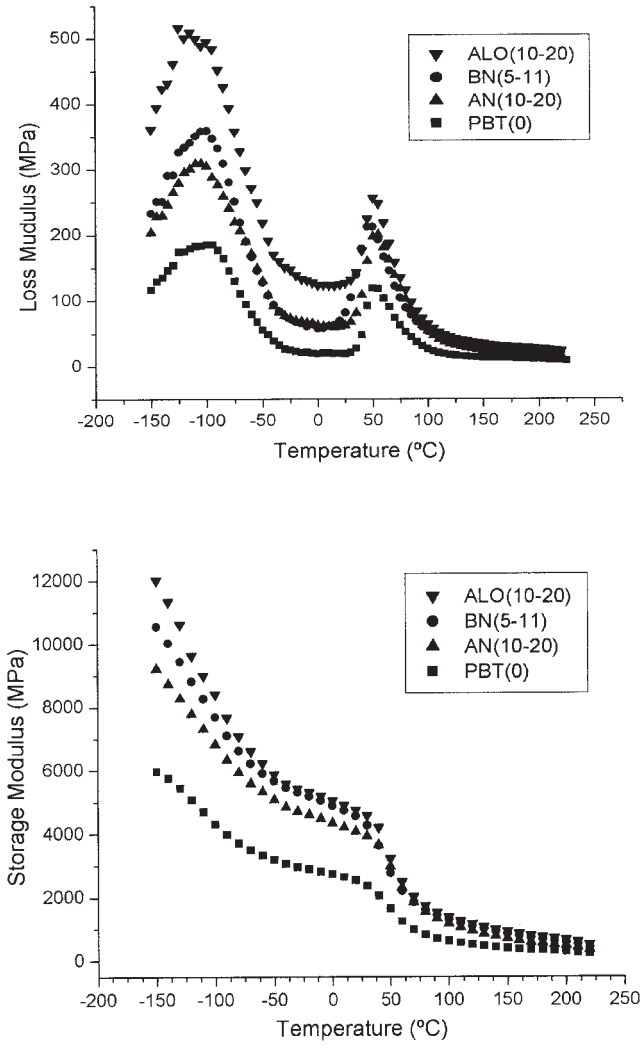

Figure 8 Loss and storage moduli of (■) PBT(0), (▲) AN(10–20), (▼) ALO(10–20), and (●) BN(52) composites at 1 Hz.

$$\log a_t = \frac{-C_1(T - T_0)}{C_2 + (T - T_0)} \quad (1)$$

where a_t is the shift factor, T_0 is the reference temperature, T is the temperature of interest, and C_1 and C_2 are constants. This type of behavior appears curved in an Arrhenius plot of ln f versus $1/T$. However, crystalline polymers with limited amorphous domains exhibit Arrhenius behavior, as noted here.[45,46] The temperatures for the β relaxation at 1 Hz correspond well to the glass transitions determined by temperature-modulated DSC at scanning rate of 3°C/min with an amplitude of 1°C.

For each sample, two straight lines have been obtained: one for the β transition (high temperature) and another for the γ transition (low temperature). The activation energies for the β and γ relaxations of filled PBT samples were calculated from Arrhenius plots and are shown in Table IV. Because the β transition is associated with large-scale motions of the polymer chain, it is reasonable that the activation energies of the β transition are higher than those of the γ transition, which involves the local motions of chemical groups, such as carbonyl[42] and glycol.[41] The activation energies for the β and γ transitions of filled polymers are higher than that of the pure PBT sample. The increase in the activation energy indicates that most of the fillers either mechanically constrain the motion of polymer chains and side groups or bind to the polymer matrix.

CONCLUSIONS

CBT oligomers were blended with a variety of ceramic fillers, including: BN, AN, and Al_2O_3. The low melt viscosity allowed for excellent blending, as depicted by SEM micrographs. The blends were polymerized to yield PBT/filler composites. The effects of the filler type and composition on the composite thermal and mechanical properties as well as the morphology were examined. It was determined that the melting/crystallization temperatures were only slightly affected by the addition of ceramic fillers. In addition, the onsets of thermal decomposition in air for pure PBT and PBT/filler composites were virtually identical at 370°C. These results demonstrate the high thermal stability of PBT-based underfill materials. The mechanical properties depended on both the filler type and the degree of crystallinity of the polymer matrix. A significant decrease in CTE was observed for BN-filled samples, which in turn possessed the lowest CTE value of the filler itself. CTE also decreased with an increase in the crystallinity percentage of the PBT matrix. Similarly, the storage modulus for each composite was correlated to Young's modulus of the pure fillers as well as the crystallinity percentage of the polymer matrix.

References

1. Wong, C. P. Advances in Polymer Science; Springer: Berlin, 1988; Vol. 84, p 63.
2. O'Malley, G.; Giesler, J.; Machuga, S. IEEE Trans Component Packaging Manufact Technol Part B 1994, 17, 248.
3. Rimdusit, S.; Ishida, H. Polymer 2000, 41, 7941.
4. He, Y.; Moreira, B. E.; Overson, A.; Nakamura, S. H.; Bider, C.; Briscoe, J. F. Thermochim Acta 2000, 357, 1.
5. Lau, J. H. Chip on Board; Van Nostrand Reinhold: New York, 1994; p 504.
6. Wada, M. IEEE/IMC Proc 1998, 56.
7. Machuga, S. C.; Lindsey, S. E.; Moore, K. D.; Skipor, A. F. Proc IEEE/CHMT Int Electron Manufact Technol Symp 1992, 53.
8. Barber, I. G. U.S. Pat. 5,700,723 (1997).
9. Todd, M. G. U.S. Pat. 5,654,081 (1997).
10. Osuna, J. A.; Dershem, S. M. U.S. Pat. 5,714,086 (1998).
11. Okura, J. H.; Darbha, K.; Shetty, S.; Dasgupta, A.; Caers, J. F. J M Proceedings, Electronic Components & Technology Conference 1999, 49, 589.
12. Wong, C. P.; Shi, S. H.; Jefferson, G. Proc ECTC 1997, 47, 850.
13. Vo, H. T.; Todd, M.; Shi, F. G.; Shapiro, A. A.; Edwards, M. J Microelectron 2001, 32, 331.
14. Ishida, H.; Rimdusit, S. Thermochim Acta 1998, 320, 177.
15. Bujard, P.; Kuhnlein, G.; Shiobara, T. IEEE Trans Component Packaging Manufact Technol Part A 1994, 17, 527.
16. Lu, X.; Xu, G. J Appl Polym Sci 1997, 65, 2733.
17. Wong, C. P.; Bollampally, R. S. J Appl Polym Sci 1999, 74, 3396.
18. Xu, Y.; Chung, D. D. L.; Mroz, C. Compos A 2001, 32, 1749.
19. Danes, F.; Garnier, B.; Dupuis, T. Int J Thermophys 2003, 24, 771.
20. Agari, Y.; Tanaka, M.; Nagai, S. J Appl Polym Sci 1987, 34, 1429.
21. Ng, H. Y.; Lau, S. K.; Lu, X. Mater Sci Forum 2003, 437, 239.
22. Kuang, J.; Zhang, C.; Zhou, X.; Wang, S. J Cryst Growth 2003, 256, 288.
23. Jayathilaka, P. A. R. D.; Dissanayake, M. A. K. L.; Albinsson, I.; Mellander, B. E. Electrochim Acta 2002, 47, 3257.
24. Wang, Y. F. U.S. Pat. 6,420,048 (2002).
25. Wang, Y. F. U.S. Pat. 6,436,549 (2002).
26. Royall, P. G.; Kett, V. L.; Andrews, C. S.; Craig, D. Q. M. J Phys Chem 2001, 105, 7021.
27. Illers, K. H. Colloid Polym Sci 1980, 258, 117.
28. Hobbs, S. Y.; Pratt, C. F. Polymer 1975, 16, 462.
29. Yeh, J. T.; Runt, J. J Polym Sci Part B: Polym Phys 1989, 27, 1543.
30. Yasuniwa, M.; Tsubakihara, S.; Ohoshita, K.; Tokudome, S. J Polym Sci Part B: Polym Phys 2001, 39, 2005.
31. Nichols, M. E.; Robertson, R. E. J Polym Sci Part B: Polym Phys 1992, 30, 755.
32. Kim, J.; Nichols, M. E.; Robertson, R. E. J Polym Sci Part B: Polym Phys 1994, 32, 887.
33. Stein, R. S.; Misra, A. J Polym Sci Polym Phys Ed 1980, 18, 327.
34. Ludwig, H. J.; Eyerer, P. Polym Eng Sci 1988, 28, 143.
35. Yokouchi, M.; Sakakibara, Y.; Chatani, Y.; Tadokoro, H. Macromolecules 1976, 9, 266.
36. Datye, V. K.; Taylor, P. L. Macromolecules 1985, 18, 671.
37. Apostolov, A. A.; Fakirov, S.; Stamm, M.; Patil, R. D.; Mark, J. E. Macromolecules 2000, 33, 6856.
38. Apostolov, A.; Fakirov, S.; Pavlov, M. J Mater Sci Lett 2002, 21, 145.
39. Leung, W. P.; Choy, C. L. J Appl Polym Sci 1982, 27, 2693.
40. Illers, K. H.; Breuer, H. J Colloid Sci 1963, 18, 1.
41. Reddish, W. Trans Faraday Soc 1950, 46, 459.
42. Chang, E.; Slagowski, E. L. J Appl Polym Sci 1978, 22, 769.
43. Nielsen, L. E.; Landel, R. F. Mechanical Properties of Polymers and Composites, 2nd ed.; Marcel Dekker: New York, 1994, p 131.
44. Polymer Physics; Gedde, U. W., Ed.; Chapman and Hall: New York, NY, 1995, p 298.
45. Seitz, J. T.; Balazs, C. F. Polym Eng Sci 1968, 151.
46. Ferry, J. D. Viscoelastic Properties of Polymers; Wiley: New York, 1961; p 235.